Density Functional Theory Studies of the Metal-Insulator Transition in Vanadium Dioxide alloys

*Haichang Lu[1], John Robertson[1]**

[1]Department of Engineering, Cambridge University, Cambridge CB2 1PZ, United Kingdom
Email: jr214@cam.ac.uk

VO_2 is of great interest because it has a metal-insulator transition involving a change in structure and electronic structure. For certain applications, it is useful to vary the band gap and the transition temperature. Although strain can be used, another method is to alloy VO_2 with oxides such as GeO_2 or MgO. Here, we carry out density functional supercell calculations on these alloys. The band gap of the alloys changes because the band edges of the M_1 phase consist of V 3d bands, where V is 6-fold bonded. However, there is also a 5-fold VO_2/MgO structure with a much larger band gap of up to 2.1eV. For Ge alloying, the structure reverts to the rutile phase but with a band gap, because GeO_2 has a rutile phase. We also find that hydrogen doping varies the oxide gap between 0eV to 1eV. The result is consistent with experimental observations and it gives an important view to explain the mechanism of alloying.

1. Introduction

Vanadium dioxide (VO_2) has been intensively studied due to its metal-insulator transition (MIT) at 340K, between a high-temperature metallic rutile phase and a low temperature insulating monoclinic phase [1-3]. Potentially, VO_2 can be used as a thermochromic material in smart windows [4], in optical [5] or RF switches [6,7] and steep slope transistors [8,9]. VO_2 is a strongly-correlated material which makes it useful for optoelectronics [5]. However, the MIT involves structural and magnetic order changes which are still debated due to the complexity of correlated oxide systems [1,3,10]. Experimentally, the magnetic order and structure are hard to obtain. For theory, it is debated to what extent density functional theory describes the nature of the MIT. Here, we describe how the band gap opens and closes during the MIT and its relation to the spin and the structural pairing of vanadium.

VO_2 can be more useful if its phase-change temperature T_C, as well as insulating phase gap, can be varied. For example, if T_C is near to the room temperature, and the direct band gap lies within the visible spectrum range, then VO_2 is useful for window coatings for indoor temperature control [4]. Various experimental reports show that alloying MgO can widen the band gap and alloying with GeO_2 can increase the phase-change temperature [11-13]. However, there is no full explanation of these effects in simulation and some simulations show no increase for the band gap [12]. Here, we find that the band gap cannot change by simply substitution because the band edge is made purely of V 3d states. Therefore, Mg is not a dopant but an agent to reconstruct the bonding of vanadium, which explains why a high content of MgO is needed and why Mg is most suitable, not Al or Fe, etc. Secondly, we found that alloying with GeO_2 actually converts VO_2 back to rutile structure but into an anti-ferromagnetic insulating phase.

2. Methods

Density functional theory (DFT) has been widely used to describe VO_2 at its most simple, but it fails to give a band gap for the M1 phase [1]. The local density approximation (LDA) or generalized gradient approximation (GGA) can be improved by adding an on-site repulsive term U for V 3d states [14]. The more expensive GW method combined with dynamic mean field

theory (DMFT) can reproduce the correct electronic structure [3]. However they are unsuitable for the large unit cells needed for alloy studies. Eyert [1,10] noted that the lower cost hybrid functional methods such as the Heyd-Scuseria-Ernzerhof (HSE) functional could give a reasonable band-like description of the electronic states. Rubio et al [15] notes that the inclusion of nonlocal exchange rather than strong correlations are the key factor to cure the band gap error of LDA. However, this proposal was dented when Schwingenschlögl [16] claimed that hybrid functionals gave the incorrect magnetic ground states for both phases. More recently, Pantelides et al [17] noted that hybrid functionals containing a lower fraction of exact exchange, with a better O potential, would work. We have found elsewhere that the GGA+ U method will give similar results to hybrid functional for some cases, so we use this method to study the atomic and electronic structure of the alloys.

The calculations were performed using CASTEP plane wave density functional code [18]. The Perdew-Burke-Ernzerhof (PBE) form of the GGA including the U is used for the electron exchange-correlation functional. Ultra-soft pseudopotentials with a plane wave cut-off energy of 340eV are used. The geometry optimization algorithm uses the Two-Point-Steepest-Descent (TPSD) for an initial rapid search of atomic structure, followed by Broyden-Fletcher-Goldfarb-Shanno (BFGS) method for accurate structure calculation [18]. The relaxation is performed until the residue force is lower than 0.03eV/Å. Values of U from 2eV to 3.25eV were tested and finally U = 2.5 eV was used. The density of k-point sampling varies for different cell size and is illustrated in the result part. All calculations are spin-polarized but spin-orbit coupling is excluded.

3. Results

3.1. Pure VO_2: from Rutile to M_1 phase

We calculated each phase's structure, magnetic order and partial density of states (PDOS). Fig 1(a) shows how the monoclinic M_1 phase can be formed from two primitive cells of the rutile phase. The M1 structure is formed by pairing V atoms along the z-direction to form two identical V-V chains. This leaves two kinds of O atoms. The V-O_1 bond is longer than the V-O bond in rutile phase while the V-O_2 bond is shorter. The space group changes from $P4_2/mnm$ to $P2_1/c$. The lattice constants of each phase are given in Table 1 with other calculation reports for comparison. A 3x3x3 k-point is used for the PDOS calculation.

Table 1 Calculated lattice constants of various VO_2 phases compared to previous work.

Lattice	Rutile		M_1	
constant (Å)	This work	others	This work	Ref[1]
a	4.62	4.55	5.67	5.75
b	4.62	4.55	4.61	4.54
c	2.78	2.85	5.44	5.38
α	90.00	90.00	90.00	90.00
β	90.00	90.00	122.13	122.65
γ	90.00	90.00	90.00	90.00

The opening and closing of the band gap during the MIT is widely considered to be due to the structural change. However, we found that, most importantly, the gap is induced by the spin-

pairing along the V chains which splits the $d_{//}$ states shown in Fig. 1(b). This is because a gap is present in the rutile structure if it has anti-ferromagnetic (AFM) order, (unlike experimentally). On the other hand, a non-magnetic monoclinic phase is gapless.

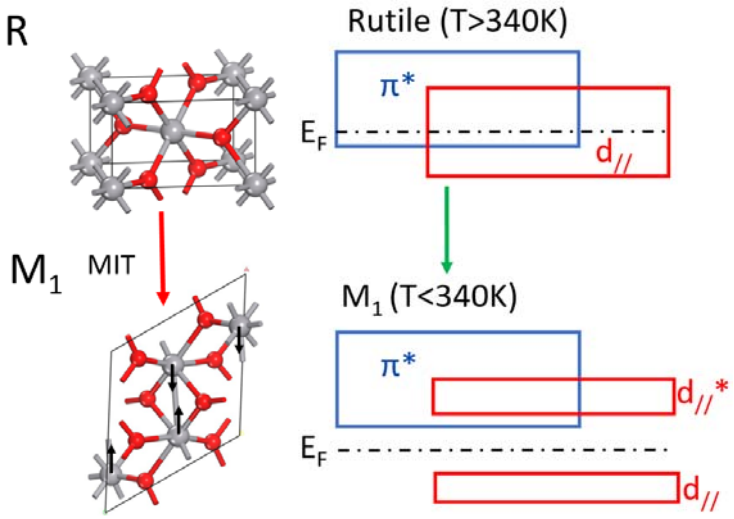

Figure 1. (a) Structure, spin pairing of the rutile and M1 phase. In the M1 phase, there is strong coupling along the vertical V-V chain, and weak coupling laterally between chains. (b) band diagram of the R and M1 phases, showing the band gap opening up in the $d_{//}$ states.

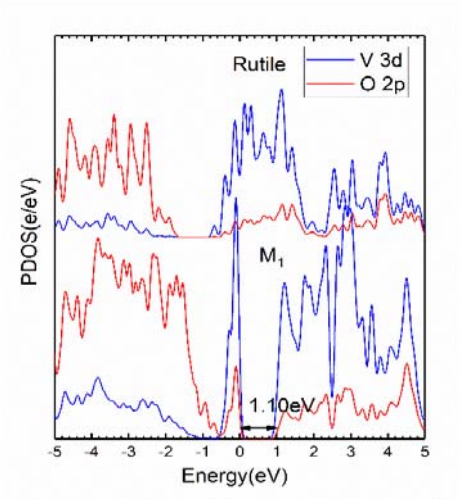

Figure 2. Partial density of states (PDOS) of the non-magnetic R phase and AFM M1 phase of pure VO_2.

The cell size of M_1 is double that of the rutile primitive cell. Two vanadium atoms then pair up to form a V-V chain. We found that the magnetic order in M_1 should be AFM, where the chained vanadium atoms have the opposite spin direction, while the vanadium atoms on adjacent chains have the same direction of spin, as shown in Fig. 1(a). The two chained vanadium atoms with opposite spins are strongly coupled while the two adjacent vanadium atoms with the same spin direction are weakly coupled. In the high-temperature rutile phase, the magnetic order is paramagnetic or non-magnetic, as discussed elsewhere.

A band gap of 1.10eV is calculated in GGA+U for the M_1 phase and there is a small 'gap' between vanadium's d bands in the valence band and oxygen p bands, as in Eyert [1] (Fig. 2). For each V-V chain, there is one d band in the valence band (VB) known as $d_{//}$ because the orbital is parallel to the chain direction, and nine d bands in the conduction band (CB) which consist of both $d_{//}$* and π*. These results are consistent with Goodenough's model [2].

3.2 Mg alloying

MgO alloying is one of the main ones studied experimentally [11]. MgO is of interest being a highly ionic oxide with a large band gap of 7.4 eV, which gives no states near the Fermi level in the alloys. In this work, we choose the alloying ratio of 25% which is high and the compound is MgV_3O_7.

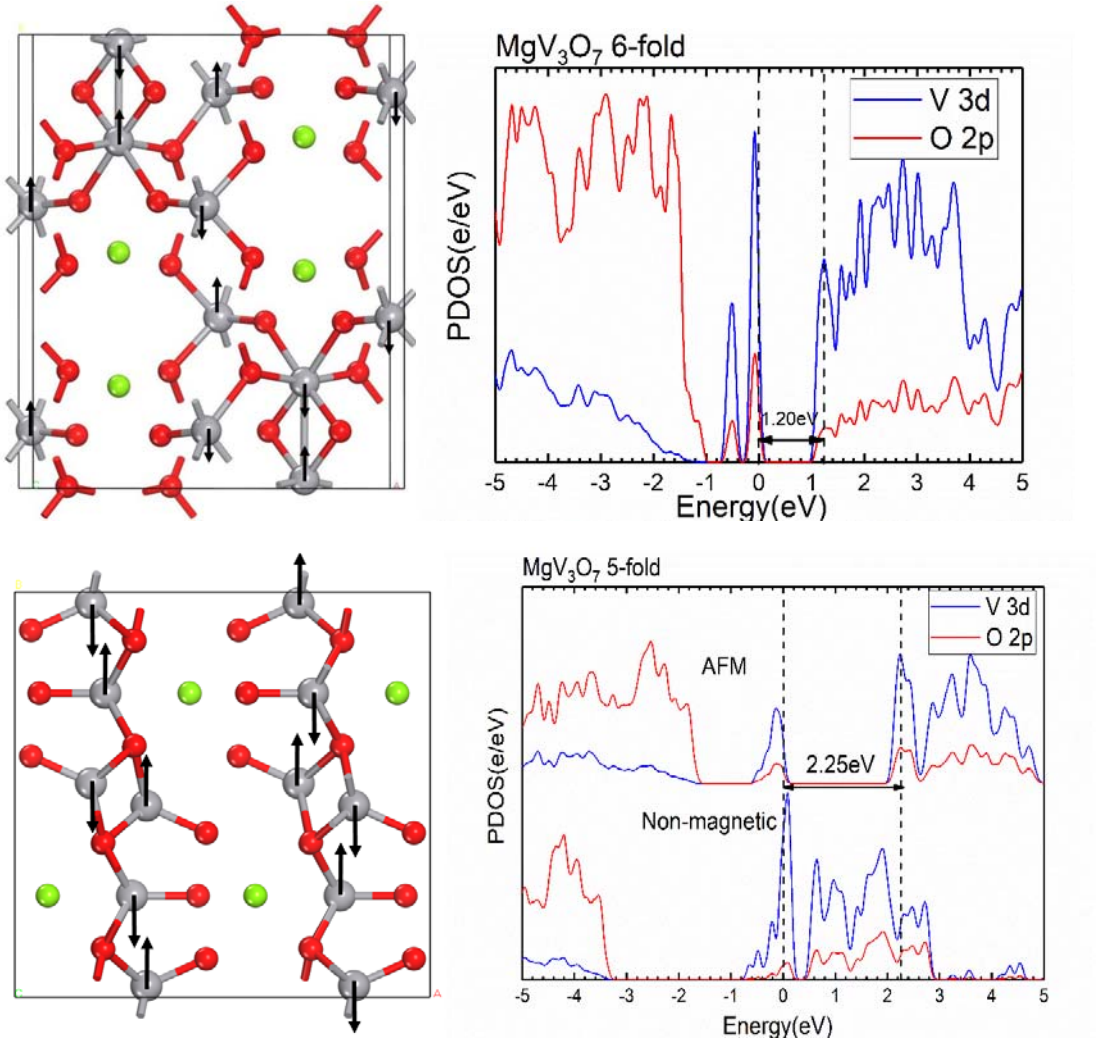

Figure 3. Structure, spin order and PDOS of MgO alloying VO_2. (a,b) for the 25% MgO phase with 6-fold V sites; (c,d) for the 25% MgO phase with 5-fold V sites.

We use a 1x1x3 k-point mesh. Half of the V-V chains break due to the larger cell size after inserting the MgO. The spin coupling is smaller, but the spin-order is still AFM. The d band at

the VBM splits due to symmetry breaking, but the ratio of occupied and unoccupied d bands and the band gap are not changed as V is still 6-fold bonded for V-O bonds. This result is in consistent with experiment where the band gap widens to 2.32eV for 19% alloying [11]. As the MgO content is quite high, it is possible that the structure undergoes a reconstruction. A crystal search [19] found that a new structure with 5-fold V-O bonds has lower energy than the previous structure by 0.43eV per VO_2 formula unit (FU). The symmetry is higher to PNMA and the gap rises from 1.2eV to 2.25eV. The rearrangement helps Mg to distribute among the cell which is reasonably preferred to the one with 6-fold V's, where two Mg atoms are paired together. The spin-order remains AFM during the reconstruction and the spatial separation of each spin-paired V gets small enough to allow a stronger coupling. To find whether the new structure can switch phases, we calculated the PDOS of the non-magnetic 5-fold MgV_3O_7 structure and find that it is gapless (Fig 3b).

Among all other possible alloys like Al (Al_2O_3), Si (SiO_2), Fe (Fe_2O_3), Mg (MgO) is the most favored because no Mg-O valence bond is formed in such a highly ionic compound. Therefore, the Mg atom locations can be varied, changing the V-O bonding, while keeping the stoichiometry. Apart from MgV_3O_7, MgV_2O_5 and MgV_4O_9 can exist with similar band gaps, bonding, and spin order.

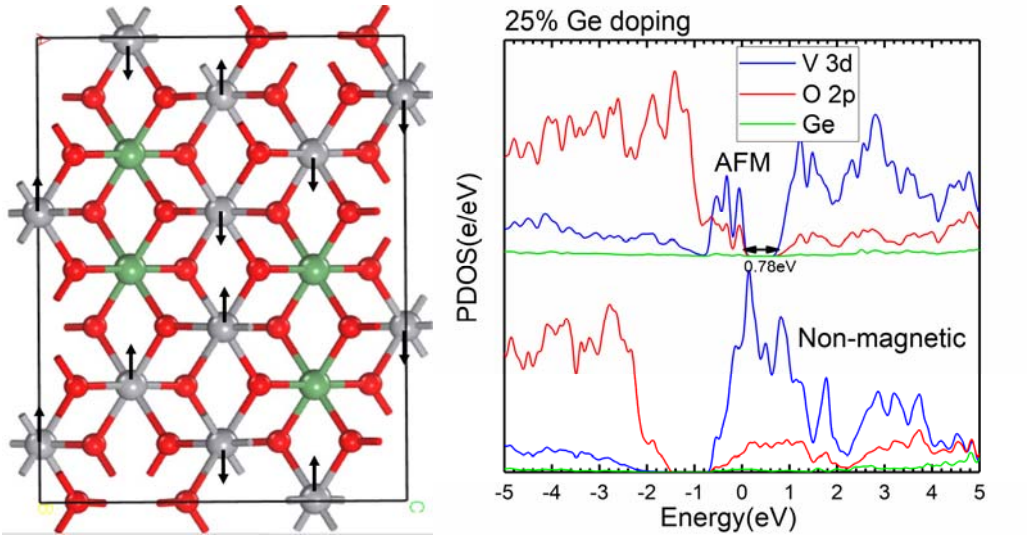

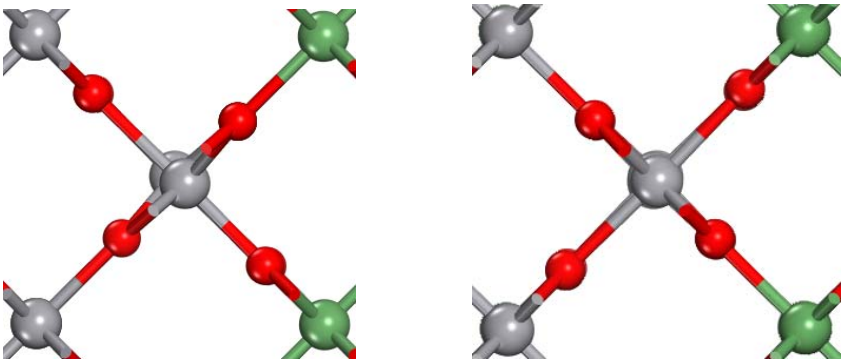

Before relaxation

After relaxation

Figure 4. (a) Structure and spin order of 25% GeO_2 alloying in VO_2. PDOS for the antimagnetic and non-magnetic phases of the 2% MgO alloy. (c,d) The side view of the alloying structure before and after geometry relaxation.

3.3 Ge alloying

We have also calculated the case of alloying with tetravalent Ge. A 25% GeO_2 alloy (GeV_3O_8) is shown in Fig. 4. We initialize with AFM ordering and find that AFM is kept during relaxation and a gap of 0.78eV is obtained. Unlike MgO, the alloy structure returns from M_1 to rutile, as shown in Fig. 4 (c) and (d), where the side view shows that the M_1 type deformation disappears as Ge is doped. This is because GeO_2 has a metastable rutile phase which allows the alloy to revert to rutile. However, the spin-order, as shown previously, is relatively independent of structural order. If the temperature is low enough, the first order symmetry-breaking will happen. Therefore, AFM is still maintained in a low-temperature phase. We then predict that by controlling the amount of Ge doping, we can control the phase change temperature. A calculation of the total energy with the non-magnetic and AFM spin ordering finds that the energy difference between the metallic and non-metallic phases increases slightly, equivalent to a rise in transition temperature, as observed experimentally [13].

Fig. 4 (a) shows the spin ordering for the VO_2:GeO_2 alloy. Unlike the insulating phase of pure VO_2, spin pairing along the z-axis occurs without any structural pairing of V-V sites. The structure here assumes Ge atoms lie on one of the two chains. The spin-pairing is weakened as a result of the overall spatial separation of V, thus reducing the gap to 0.78eV. Krammer [13] shows that the transition temperature can be raised by Ge doping, indicating the magnetic ground state energy is lower.

Generally, the spin alignment appears to depend on the location of the dopant atoms within the chains of V sites, so that the V sites can pair up antiferromagnetically. However, the V pairing is able to occur for various spatial orderings of the dopant atoms. Thus VO_2 (unlike V_2O_3) is not so sensitive to disorder, as noted both experimentally or theoretically [14,20].

3.4 Hydrogen

The final dopant considered is hydrogen. This is unlike the others, in that it can be intercalated into an existing solid so the lattice only undergo limited re-arrangements [21]. In semiconductors, hydrogen has two basic responses, it can be deep amphoteric impurity or a shallow donor [22,23]. Hydrogen acts as a shallow donor in many rutile phase oxides such as TiO_2 and SnO_2. Our calculations show that hydrogen acts similarly in VO_2. It lies above the bonding plane of the O site, and forms an O-H bond, with a slight puckering effect on the O site's geometry. Fig 5(a) shows the geometry for the undoped M1 phase, as an insulator, with E_F in the gap, Fig 5(b). Fig 5(c) shows the geometry 50% hydrogen doped ordered alloy. The Fermi level has moved well into the conduction band lying above the $d_{//}$* state. Chen et al [21] have noted that this behavior is confirmed by synchrotron studies, in terms of core level shifts and conductivity changes.

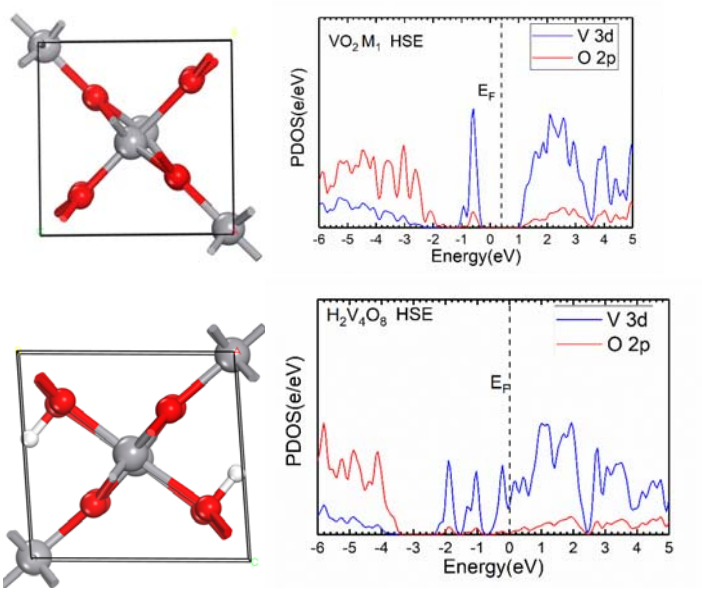

Fig. 5(a,b) geometry and band structure of thr M1 phase of pure VO_2 using HSE. (c,d) geometry and band structure of hydrogen doped VO_2, with the Fermi level in the conductiuon band.

4. Conclusion

The structure and electronic structure of pure insulating VO_2 and alloyed VO_2 are calculated. The ground state of the VO_2 M_1 phase is anti-ferromagnetically ordered with strong spin-coupling occuring along chains of V sites. The alloying of MgO can double the band gap from 1.1eV to 2.2eV by a structure rearrangement, while the substitutional doping with tetravalent Ge can return the insulating phase to the rutile structure. This work provides a detailed theoretical view to explain the experimental observation and is important in the application of VO_2 in smart coatings and MEMS.

References

[1] V. Eyert, *Ann. Phys. (Leipzig)* **2002**, 11, 9.
[2] J. B. Goodenough, *J. Solid. State Chem.* **1971**, 3 490.
[3] K. Liu, S. Lee, S. Yang, O. Delaire and J. Wu, *Materials Today* **2018**, 21 875.
[4] S. Wang, M. Liu, L. Kong, Y. Long, X. Jiang and A. Yu, *Prog. Mater Sci.* **2016,** 81, 1-54
[5] P. Markov, R. E. Marvel, H. J. Conley, K. J. Miller, R. F. Haglund, Jr. and S. M. Weiss, *ACS Photonics*, **2015**, 2, 1175-1182.
[6] W A Vitale, L Petit, C F Moldovan, M Fernandez, A Paone, A Schuler, A M Ionescu, Sensors Actuators A 241 245 (2016);
[7] E A Casu, N Oliva, M Cavalieri, A A Muller, A Fumarola, W A Vitale, A Krammer, A Schuler, M Fernandez, A M Ionescu, IEEE J EDS 6 965 (2018);
[8] N. Shukla, A. V. Thathachary, A. Agrawal, H. Paik, A. Aziz, D. G. Schlom, S. K. Gupta, R. Engel-Herbert and S. Datta, *Nat. Communication*, **2015**, 6, 7812.
[9] W A Vitale, E A Casu, A Biswas, T Rosca, C Alper, A Krammer, G V Luong, O T Zhao, S Mantl, A. Schuler, A M Ionescu, Sci Reports 7 355 (2017)

[10] V. Eyert, *Phys. Rev. Lett.* **2011**, 107, 016401.
[11] S. Hu, S. Li, R. Ahuja, C. G. Granqvist, K. Hermansson, G. A. Niklasson and R. H. Scheicher, *Appl. Phys. Lett.* **2012**, 101, 201902.
[12] S. Li, N. R. Mlyuka, D. Primetzhofer, A. Hallén, G. Possnert, G. A. Niklasson and C. G. Granqvist, *Appl. Phys. Lett.* **2013**, 103, 161907.
[13] A. Krammer, A. Magrez, W. A. Vitale, P. Mocny, P. Jeanneret, E. Guibert, H. J. Whitlow, A. M. Ionescu and A. Schüler, *J. Appl. Phys.* **2017**, 122, 045304.
[14] C Weber, D R O'Regan, N Hine, M C Payne, G Kotliar, P B Littlewood, Phys Rev Lett 108 256402 (2012)
[15] F. Iori, M. Gatti and A. Rubio, *Phys. Rev. B.* **2012**, 85 115129.
[16] R. Grau-Crespo, H. Wang and U. Schwingenschlögl, *Phys. Rev. B.* **2012**, 86, 081101.
[17] S. Xu, X. Shen, K. A. Hallman, R. F. Haglund Jr. and S. T. Pantelides, *Phys. Rev. B.* **2017**, 95, 125105.
[18] S. J. Clark, M. D. Segall, C. J. Pickard, P. J. Hasnip, M. J. Probert, K. Refson and M. C. Payne, *Z. Kristallogr.* **2005**, 220, 567.
[19] S Jain et al, APL Materials 1 011002 (2013)
[20] J G Ramirez, T Saarbeck, S Wang, J Trastoy, M Mainou, J Lesueur, J P Crocombette, J E Villegas, I K Schukker, Phys Rev B **9**1 205123 (2015)
[21] S Chen, Z Wang, L Fan, Y Chen, H Ren, H Ji, D Natelson, Y Huang, J Jiang, C Zou, Phys Rev B 125130 (2017)
[22] P W Peacock, J Robertson, Appl Phys Lett 83 2025 (2003)
[23] H Li, J Robertson, J Appl Phys 115 203708 (2014)